Presented at the 24th European PV Solar Energy Conference and Exhibition, 21-25 September 2009, Hamburg, Germany

LIFETIME STUDIES ON CRYSTALLINE SILICON THIN-FILM MATERIAL BY PHOTOLUMINESCENCE IMAGING

Fabian Kopp, Philipp Rosenits, Thomas Roth, Evelyn Schmich, Stefan Reber, Wilhelm Warta
Fraunhofer Institute for Solar Energy Systems (ISE)
Heidenhofstrasse 2, D-79110 Freiburg, Germany
Phone: +49 761 4588 5661, Fax: +49 761 4588 9250, Email: fabian.kopp@ise.fraunhofer.de

ABSTRACT: In this paper it is demonstrated how photoluminescence imaging (PLI) can serve to qualitatively and quantitatively characterize the properties of an epitaxial silicon layer. In the first part a set of microelectronic-grade samples is characterized electrically by determining the epitaxial layer lifetime. In the second part a set of samples for photovoltaic application is studied. In this case the focus is on the possibilities for a qualitative analysis of the thickness inhomogeneity of the epitaxial layer.
Keywords: Thin-film, Photoluminescence, Lifetime

1 INRODUCTION

The Epitaxial Wafer Equivalent (EpiWE) solar cell concept is based on an inexpensive highly doped (N_{Dop}>10^{18} cm^{-3}) silicon substrate on which a moderately doped (N_{Dop}~10^{16} cm^{-3}) epitaxial silicon layer is deposited by means of chemical vapor deposition (CVD). The epitaxial layer forms the base of the solar cell and has a thickness in the magnitude of about 20 µm. The substrate has a thickness in the magnitude of some 100 µm which gives the solar cell mechanical stability. Furthermore, it is crystalline, because the epitaxial silicon adopts the crystallographic structure of the substrate. The high substrate doping allows for majority carriers to flow to the metal contact on the back side through the high substrate thickness without excessive resistive losses. Moreover, the doping difference between epitaxial layer and substrate generates a band bending which is called back surface field (BSF). In the BSF region the minority carrier density is strongly reduced, so that excess carrier losses from the epitaxial layer into the substrate and recombination at the interface are reduced.

A key parameter for the performance of a finished solar cell is the excess carrier lifetime which characterizes the material quality of the electrically active layer. Consequently, an easy and reliable method to determine this excess carrier lifetime is of enormous interest for both practical process control and evaluation of the potential and limitations of the EpiWE solar cell concept. Unlike standard silicon wafer characterization, for which lifetime measurement methods, such as quasi-steady-state photoconductance (QSSPC) [1] or quasi-steady-state photoluminescence (QSSPL) [2] are common, similar characterization methods for crystalline silicon thin-films are still lacking.

2 MEASUREMENT AND ANALYSIS PRINCIPAL

The PLI [2] measurement principle is based on emission of photons due to direct radiative recombination of excess carriers constantly generated by a laser diode. The measurement setup can be seen in Figure 1. A homogenization optics converts the narrow light beam coming out of the laser fiber into a flat profile, which is homogeneous over 15.6×15.6 cm^2. The maximum excitation intensity is about 0.2 W/cm^2 and as the excitation wavelength is λ=790 nm, which is equivalent to an absorption length of L_{abs}=13 µm in silicon, most of the excess electron-hole pairs are generated in the epitaxial layer if the layer thickness is greater than L_{abs}. A CCD camera counts the number of detected PL photons spatially resolved.

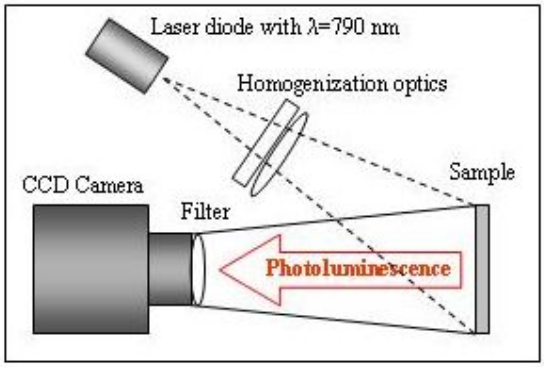

Figure 1: PLI measurement setup at Fraunhofer ISE. The light excitation and PL detection happens on the same side of the sample.

The PL intensity I_{PL} is in general given by the excess carrier profile $\Delta n(z)$, the doping profile $N_{Dop}(z)$ and the doping dependent coefficient of the radiative recombination rate $B(n(z),p(z))$ [3]

$$\begin{aligned} I_{PL} &= A_i \cdot U_{rad} \\ &= A_i \cdot \int B(n(z),p(z)) \cdot n(z,t) \cdot p(z,t) dz \\ &\approx A_i \cdot \int B(n(z),p(z)) \cdot [N_{Dop}(z) + \Delta n(z,t)] \Delta n(z,t) dz \end{aligned} \quad (1)$$

The calibration factor A_i contains optical properties of the sample like reflectance and surface texture. In comparison the calibration factor of a wafer can be determined by a so-called self consistent calibration [4]. This is not possible in the way for a two layer system, because the excess carrier and dopant densities are depth dependent. The resulting PL signal consists of PL intensity contributions of both layers. Each layer refers to a separate volume lifetime.

A new method for a quantitative determination of the excess carrier density was recently introduced [5]. The analysis principle is based on a comparison between a measured photoluminescence intensity ratio and

associated simulated radiative recombination ratios for samples with different epitaxial layer thicknesses. It benefits from the fact that for low excess carrier lifetimes within the epitaxial layer the carrier concentration in the said layer is limited by bulk recombination, while for high carrier lifetimes surface and interface recombination between epitaxial layer and substrate is dominating. This property means that in general a correlation between epitaxial layer thickness and photoluminescence intensity exist. For the calculation of the rate of radiative recombination an excess carrier profile is simulated with the tool PC1D [6].

An exact determination of the sample parameters is especially important, because differences in epitaxial layer thickness and doping have a high impact on the simulated excess charge carrier profile and thus on the computed PL intensity. Accordingly, dopant density profiles were determined with the spreading resistance profiling technique SRP. This technique is based on a low voltage measurement of the spreading resistance between two point contacts [7]. The dopant profile obtained gives information about the dopant density which is mainly constant in each layer. Additionally, the abrupt dopant density step between epitaxial layer and substrate defines the epitaxial layer thickness and a 2 to 3 µm deep tail of dopant density from the substrate into the epitaxial layer coming from out diffusion during the CVD process is identified.

3 SAMPLE PREPARATION OF MICROELECTRONIC-GRADE SAMPLES

The investigated microelectronic-grade lifetime samples were manufactured on high-purity 6" boron-doped Czochralski (Cz) substrates with a [100] orientation and a thickness of around 700 µm. The backsides were sealed by a low-temperature oxide to prevent autodoping during the epitaxy, i.e. to prevent the out-diffusion of dopant atoms from the substrate into the reaction chamber and back again into the epitaxial layer. The epitaxy was realised by CVD at high temperatures around 1180°C and pressures of 80 torr. The epitaxial layer was also boron-doped. SRP measurements revealed a substrate doping concentration of $N_{Dop,Sub}$=3×10^{18} cm^{-3} and an epitaxial doping concentration of $N_{Dop,Epi}$=1.1×10^{16} cm^{-3}. The epi-layer thickness varied between 20 µm, 35 µm and 50 µm.

After the epitaxy, the wafers were laser-cut into 5×5 cm^2 samples, RCA-cleaned and subsequently surface-passivated. This was done by coating with a 70 nm SiN_x layer deposited by plasma-enhanced chemical vapour deposition (PECVD) at 350°C for 10 min.

4 RESULTS AND DISCUSSION FOR MICROELECTRONIC-GRADE SAMPLES

We measured the thin-film samples using the PLI setup described in Sect. 2. In Figure 2 a PL image of a 35 µm thick epitaxial layer is shown. The PL intensity distribution is found to be mainly laterally homogeneous, thus an averaged value of epitaxial layer thickness can be attributed to this sample. Three samples with same epitaxial thickness were measured and averaged to one resulting value.

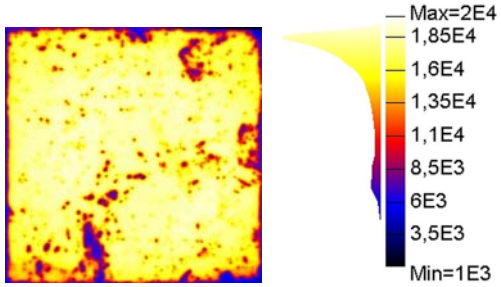

Figure 2: PL image of a 35 µm thick microelectronic-grade epitaxial layer at an excitation intensity of 0.015 W/cm^2 and an acquisition time of 60 s. Yellow areas belong to high numbers of counts whereas black areas belong to low number of counts.

The PL intensities correlated monotonically with the epitaxial layer thickness. A calculation of the PL ratios gave the value I_{50}/I_{20}=1.73 for the ratio of the measured PL intensities of the W_1=50 µm and the W_1=20 µm samples, and I_{35}/I_{20}=1.40 and I_{50}/I_{35}=1.23 for the other two combinations, respectively.

In the next step ratios of the radiative recombination rate were simulated. This rate can be calculated by an excess carrier profile which is simulated by the tool PC1D. The sample surfaces are described by recombination velocities (SRV). The SRV of the epitaxial surface can be determined by a 1 Ωcm float zone reference sample with same passivation scheme, for which a value of S_{Epi}=25 cm/s was obtained. The SRV of the substrate surface was assumed to be S_{Sub}=10000 cm/s. Although this value is high, the excess carrier profiles are not affected, because of the low bulk lifetime and high thickness of the substrate. The interface recombination is experimentally difficult to access. Preliminary studies motivated a value between S_{int}=0 cm/s and S_{int}=1000 cm/s [8], so that quantitative lifetime evaluation is done for both cases. Additionally, the excess carrier profiles are calculated for several given τ_{Epi} values. A PLI measurement of the substrate side resulted in a much lower PL intensity, because of the high substrate doping. Accordingly, the total photoluminescence signal at excitation of the epitaxial layer comes almost entirely from the epitaxial layer region. Therefore, the excess carrier density was integrated over the epitaxial layer thickness and appropriate ratios are formed.

In Figure 3 the quantitative determination of epitaxial layer lifetime is shown. Comparing measured PL intensity ratios of different epitaxial layer thicknesses to simulated ratios of the radiative recombination results in epitaxial layer lifetimes. The continuous lines represent an interface recombination velocity of S_{int}=0 cm/s and the dashed lines S_{int}=1000 cm/s. The determination results in an epitaxial layer lifetime of 15 to 66 µs.

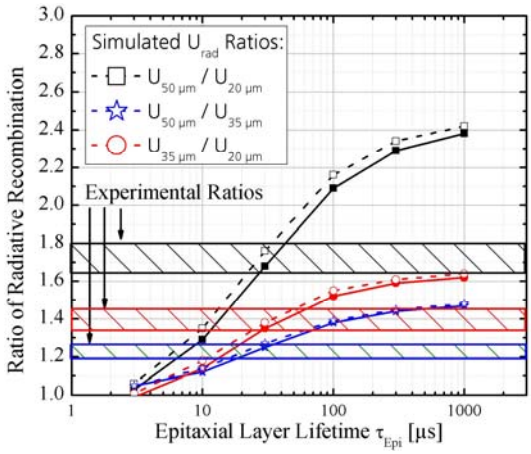

Figure 3: Experimental ratios with error margins of measured PL intensity and calibration curves which have been calculated from excess carrier profiles. If an interface recombination velocity S_{int} between 0 cm/s, continuous lines, and 1000 cm/s, dashed lines, is assumed, an epitaxial layer lifetime of 15 to 66 µs results.

5 EPITAXIAL LAYERS FOR PHOTOVOLTAIC APPLICATIONS

In the second part of this paper a set of thin-film lifetime samples deposited at Fraunhofer ISE is discussed. The deposition was done at the CVD reactor RTCVD100 [9]. Always two substrates which are located next to each other are deposited on in one run. The flux of the process gases Trichlorosilane ($HSiCl_3$) as precursor gas and Diborane (B_2H_6) for the p-type doping is laterally inhomogeneous. As a result areas of higher and lower deposition rates and thus epitaxial layer thicknesses appear. A correlation between epitaxial layer thickness and PL intensity is expected. Especially for these epitaxial layers a spatially resolved determination of the epitaxial thickness is important, because otherwise an attribution of local PL intensities is not possible. Accordingly, on the assumption of equal electrical properties in the epitaxial layer and at the surface the epitaxial thickness mapping and PL Intensity mapping correspond.

3 SAMPLE PREPARATION OF EPITAXIAL LAYERS FOR PHOTOVOLTAIC APPLICATIONS

As substrates, 730 µm thick high-purity boron-doped Cz wafers with [100] orientation and 6.5x5 cm^2 size were chosen. The edges of the substrate are located at the CVD reactor on a carrier, so that only a 5x5 cm^2 area is deposited. The average deposition rate was about 6 µm/min, the peak temperature reached 1220°C and process time between 2 and 10 min. depending on the intended epitaxial layer thicknesses of about 20 µm, 35 µm and 50 µm. The doping concentrations of the epitaxial layer and substrate were measured by SRP and are about $N_{Epi}=8\times10^{16}$ cm^{-3} and $N_{Sub}=6\times10^{18}$ cm^{-3}. After epitaxy, the wafers were RCA-cleaned and subsequently passivated with SiN_x on both sides in a high quality passivation treatment. A first determination of the epitaxial layer thickness is done by weighing the sample before and after CVD. The mass difference can directly be converted into an average epitaxial layer thickness .

4 RESULTS AND DISCUSSION OF SAMPLES FOR PHOTOVOLTAIC APPLICATION

A first measurement showed PL intensity shapes on the epitaxial and the substrate side which did not correspond to the expected epitaxial layer thickness distribution. In Figure 4 a PL image of the substrate side can be seen.

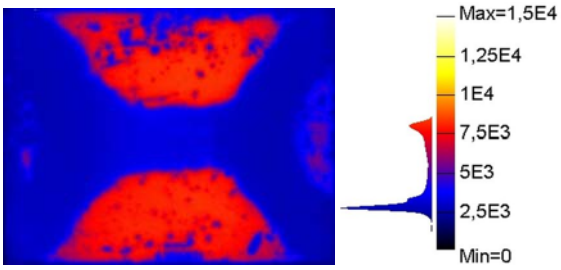

Figure 4: PL image from the substrate side of a thin-film sample at an excitation intensity of 0.015 W/cm^2 and an acquisition time of 60 s.

In comparison the intensity shape of the epitaxial and substrate side looked similar. A reference substrate, which was tempered instead of being deposited on, showed an homogeneous PL distribution and a lower PL intensity. Comparing several substrate PL images it is noticeable that the PL shapes are becoming wider with increasing average epitaxial layer thickness. The origins of the PL intensity shape are the two sample edges, which lie in between adjacent substrates during the epitaxy process.

Altogether, this first set of measurements can be explained by parasitic depositions on the substrate side. Accordingly, the samples were etched by a CP etch consisting of hydrogen fluoride, nitric acid and acetic acid to remove the parasitic depositions. In Figure 5 a PL image of the epitaxial side of an etched sample can be seen.

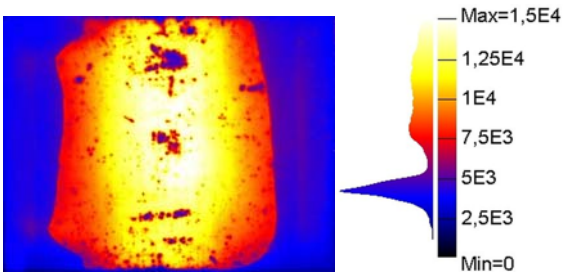

Figure 5: PL image from the epitaxial side of an etched thin-film sample at an excitation intensity of 0.015 W/cm^2 and an acquisition time of 60 s.

The PL intensity distribution looked as expected from the flow profile of the process gases. In vertical direction it is constant, but strongly decreasing towards the edges in horizontal direction. Blue sections signify low PL intensity areas equivalent to emission from the substrate and determined by the high doping density there.

To verify the correlation between the epitaxial layer thickness and PL intensity a thickness mapping is necessary. Two possible types of thickness determination

are discussed in the following.

Stacking-fault analysis is an indirect method to determine the thickness of an epitaxial layer. By measuring the edge length of a stacking fault grown on a [100] surface by means of a microscope, the height of the pyramid and therefore the epitaxial layer thickness d can be calculated according to $d = a\times(0.5)^{1/2}$, where a is the edge length of the stacking-fault [9]. An advantage of this technique is that the epitaxial layer thickness is determined and a mapping is possible. A disadvantage is that at bad surfaces stacking faults are not visible and at good material qualities only few stacking faults appear, so that a thickness mapping is not possible.

A thickness gauge can be used to determine the total sample thickness resulting in the epitaxial layer thickness by subtracting the substrate thickness. For this the substrate thickness has to be equal and known all over the sample. A mapping is possible.

A comparison of both thickness determination types resulted in a satisfying match. In general the thickness in the middle of the horizontal axis was two to three times the average value from weighting, but decreased to the edge of the horizontal axes where no epitaxial deposition took place.

After parasitic depositions were etched the surface of the epitaxial layer was rough, so that a stacking fault analysis was not possible. CP etching removes more silicon at the edges of a sample, so that uncertainties in thickness determination of the substrate occurred. As a result thickness determination by means of a thickness gauge was uncertain, but a relative thickness distribution could be obtained, see Figure 6.

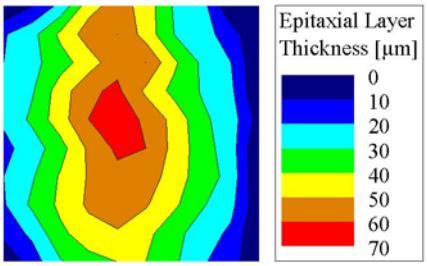

Figure 6: Thickness map of an epitaxial layer measured by thickness gauge on an etched sample. The vertical thickness distribution is approximately constant whereas horizontally a strong decrease is visible. Red areas belong to 63 to 70 µm epitaxial layer thickness and blue to 0 to 7 µm.

The PL image, Figure 5, and the thickness map, figure 6, are taken from the same epitaxial layer. For the comparison it must be pointed out that the thickness map only covers the area where silicon was deposited on, in this case 5×5 cm^2. The PL image covers the whole sample, in this case 6.5×5 cm^2. Further, in figure 5 several areas with low PL intensities due to deteriorated electrical properties like to be due to scratches and etch damages, can be seen.

5 CONCLUSION

PLI is a contactless, fast and spatially resolved measurement technique which is applicable for lifetime studies on crystalline silicon thin-films. PLI allows to resolve PL features spatially which is especially important for epitaxial layers with inhomogeneous thickness. We were able to visualize parasitic silicon depositions on the substrate side. Additionally, the epitaxial thickness distribution can directly be shown. A quantitative evaluation of the epitaxial layer lifetime is possible in principal as was demonstrated for microelectronic-grade samples.

Acknowledgements

This work has been supported by internal project funding of the Fraunhofer Society.

REFERENCES

[1] Sinton, R.A. and A. Cuevas, Applied Physics Letters, 69(17) (1996) 2510-2.

[2] Trupke, T. and R.A. Bardos, Proceedings of the 31st IEEE Photovoltaic Specialists Conference (2005) 903-6.

[3] Altermatt, P.P., et al., Proceedings of the 5th International Conference on Numerical Simulation of Optoelectronic Devices (2005) 47-8.

[4] Trupke, T., R.A. Bardos, and M.D. Abbott, Applied Physics Letters, 87(18) (2005) 184102-1- 3.

[5] Rosenits, P., et al., Proceedings of the 23rd European Photovoltaic Solar Energy Conference (2008) 2224-7.

[6] Basore, P.A. and D.A. Clugston, Proceedings of the 25th IEEE Photovoltaic Specialists Conference (1996) 377-81.

[7] Schroder, D.K., Semiconductor Material and Device Characterization. 1990, New York: John Wiley & Sons. 599.

[8] Schmich, E., High-temperature CVD processes for crystalline silicon thin-film and wafer solar cells. (2008)

[9] Bau, S., High-temperature CVD silicon films for crystalline silicon thin-film solar cells. (2003)